

Article

Emission knots and polarization swings of swinging jets

Maxim Lyutikov ^{1,*} and Evgeniya Kravchenko ²

¹ Department of Physics, Purdue University, 525 Northwestern Avenue, West Lafayette, IN 47907-2036, USA; lyutikov@purdue.edu

² Lebedev Physical Institute, Astro Space Center, Profsoyuznaya 84/32, Moscow 117997, Russia; evgenia.v.kravchenko@gmail.com

* Correspondence: lyutikov@purdue.edu

Academic Editor: Jose L. Gomez, Alan P. Marscher, Svetlana G. Jorstad

Version October 31, 2016 submitted to *Galaxies*; Typeset by L^AT_EX using class file mdpi.cls

Abstract: Knots (emission features in jets of active galactic nuclei) often show non-ballistic dynamics and variable emission/polarization properties. We model these features as emission pattern propagating in a jet that carries helical magnetic field and is launched along a changing direction. The model can reproduce a wide range of phenomena observed in the motion of knots: non-ballistic motion (both smooth and occasional sudden change of direction, and/or oscillatory behavior), variable brightness, confinement of knots' motion within an overlaying envelope. The model also reproduces smooth large polarization angle swings, and at the same time allows for the seemingly random behavior of synchrotron fluxes, polarization fraction and occasional $\pi/2$ polarization jumps.

Keywords: galaxies; active; blazars; polarisation;

1. Introduction

Blazars – a sub-class of active galactic nuclei (AGN) – have the orientation of their jets close to the line of sight (LoS). This causes their non-thermal radiation to be highly relativistically beamed. Their linear fractional polarization reaches values up to 50 per cent [e.g., 1] suggesting the presence of highly ordered magnetic fields in their compact regions [2]. Furthermore, the observed behavior of the polarization degree and angle suggest a helical shape of these magnetic fields [e.g., 2–4].

Blazars are observed to show high variability across the electromagnetic spectrum [e.g., 5,6]. The evolution of the γ -ray, optical, radio and polarized fluxes often exhibit seemingly random behavior [e.g., 7, and references therein] and in some cases might be represented by a number of isolated, individual events superimposed on a steady processes [e.g., 8,9]. In contrast, the optical electric vector position angle (EVPA) variations often show smooth swings of the linearly polarized radiation, with total rotations up to a few radians. Apparent similarities of optical flux, degree of polarization and EVPA during these events, detected in different sources and their different flaring states, suggests a common mechanism being responsible for such a behavior. The general pattern includes high variability of polarization Π , which drops to zero during the middle of an EVPA swing and then recovers back to the initial value, smooth and continuous change of polarization angle and peaked behavior of optical flux density.

2. Polarization swings: jet with helical magnetic field propagating along a variable direction

We present a model (Lyutikov & Kravchenko 2016a), shown in Fig. 1 - a jet propagating along a smoothly variable direction carrying helical magnetic field - which is able to reproduce large smooth

variations of the EVPA, yet allow for occasional sudden jumps in EVPA. In addition - and most importantly - the intensity and polarization fraction, though produced by a highly deterministic process, show large non-monotonic variations that can be mistaken for a random process. Thus, a highly deterministic set-up of the model produces both smooth variation of EVPA and yet allows for some properties of the emission to vary in a non-monotonic way, which can be interpreted as stochastic variation.

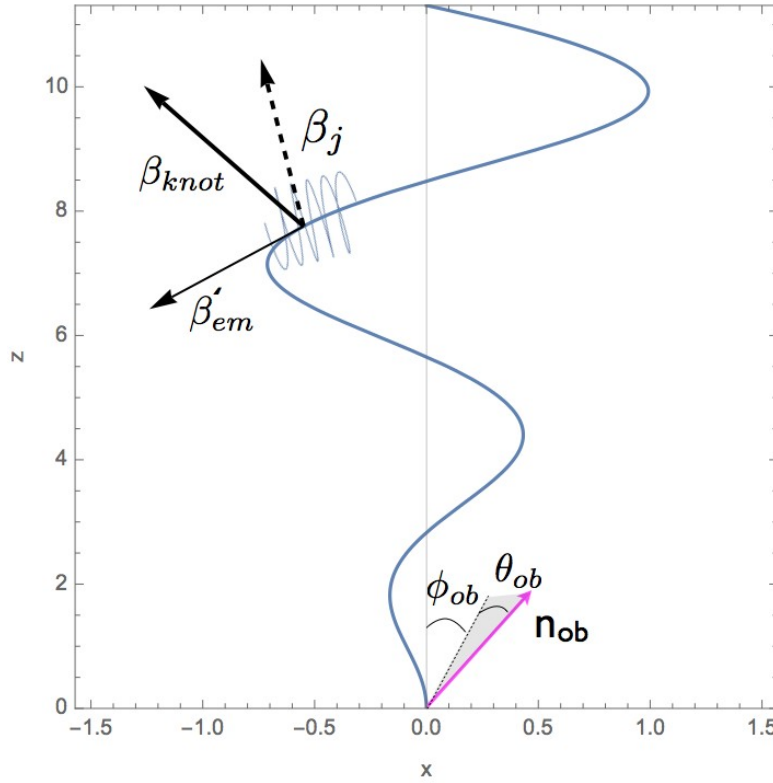


Figure 1. Schematic representation of the model. The jet is emitted along a variable direction (defined, *e.g.*, by the opening angle of the planar motion, jet's oscillation angle). Solid line is a snapshot of the jet at a given moment. Pictured is the shape of the jet at some moment t . The internal helical structure of the magnetic field within the jet is aligned with the local jet direction and changes with time. Physical motion of jet's fluid is with velocity β_j along a ballistic trajectory (dashed arrow). In addition, a feature propagates along the instantaneous direction of the jet with velocity β'_{em} (thin arrow). We assume that the feature propagates toward the core (the origin) in the jet frame. The combined ballistic motion of the fluid and of the pattern along the jet results in the non-ballistic trajectory of a pattern. Total velocity of the knot is β_{knot} - it is non-ballistic. (Velocity vectors do not form a closed triangle due to non-linearity of relativistic velocity addition.) Direction to the observer \mathbf{n}_{ob} makes angle θ_{ob} with the plane of the jet's motions; projection of \mathbf{n}_{ob} onto the plane of the jet's motion (thin dashed line) makes an angle ϕ_{ob} with respect to the symmetry axis.

We model the emitting element as a jet carrying helical magnetic field with internal pitch angle ψ , propagating with Lorentz factor γ_j . The jet produces polarized synchrotron emission. We concentrate on the optically thin region, sufficiently far downstream of the core. In terms of physical location the model is applicable to sub-parsec to parsec scale regions of the jet. In the present paper we do not make a separation between the different parts of the spectrum, *e.g.*, optical and radio, but outline the general properties of polarized synchrotron emission expected from a jet with variable direction.

Calculations of polarization produced by relativistically moving sources is somewhat complex [2,10,11]. Conventionally (and erroneously for a relativistically moving plasma!), the direction of the observed polarization for optically thin regions and the associated magnetic fields are assumed to be in one-to-one correspondence, being orthogonal to each other, so that some observers choose to plot the direction of the electric vector of the wave, while others plot vectors orthogonal to the electric vectors and call them the direction of the magnetic field. *This is correct only for non-relativistically moving optically-thin sources, and thus cannot be applied to AGN jets.* Since the emission is boosted by the relativistic motion of the jet material, *the EVPA rotates parallel to the plane containing the line of sight and the plasma velocity vector*, so that *the observed electric field of the wave is not, in general, orthogonal to the observed magnetic field*, [2,11].

In case of unresolved jets the average polarization for an axially symmetric jet can be only along or perpendicular to the jet direction. Yet the same jet can produce the average polarization along or perpendicular depending on its Lorentz factor and the viewing angle.

We consider the synchrotron emission of an unresolved, thin, circular cylindrical shell populated by relativistic electrons with a power law distribution and moving uniformly in the axial direction with constant velocity. The properties of the synchrotron emission are then determined by *three parameters*: the internal pitch angle of the magnetic field ψ , Lorentz factor of the shell in the laboratory frame γ_j and the viewing angle, θ , which the line of sight to the observer makes with the jet axis in the observer reference frame. Thus, even for fixed internal parameters of the jet, the resulting polarization signature strongly depends both on the viewing angle and the jet Lorentz factor.

The polarization direction from an unresolved jet can be either along the projection of the jet onto the plane of the sky, or perpendicular to it. Thus, as a jet's direction changes with time, the direction of polarization will also change. Most of the time, the EVPA will either be always along or across the jet. In addition, for a fairly narrow range of internal pitch angles and lines of sight a given jet can show ninety degree EVPA flips.

In Fig. 2-3 we plot the polarization signatures assuming that the motion of the jet is symmetric with respect to the line of sight and that oscillations occur between angles $-\pi/2 < \phi_j < \pi/2$ (ϕ_j is the angle between the instantaneous jet direction and the symmetry axis). We note, for $\Pi > 0$ the polarization is along the jet, while the polarization is orthogonal to the jet for $\Pi < 0$.

2.1. Overall trends and special cases

- Fastest swings of EVPA typically coincide with intensity and polarization extrema (maxima or minima).
- EVPA can experience fast $\pm\pi/2$ jumps near $\Pi = 0$. At these points intensity can be maximal or minimal.
- Swinging jets can produce very fast EVPA swings, up to $\pm\pi$; at the maximum rate of the EVPA swings (second rows in Fig. 2) the polarization fraction minima can be maximal or minimal (first rows in Fig. 2).
- Intensity depends on the EVPA and the polarization fraction in a complicated way; for accelerating jets such dependence is not necessarily symmetric.
- Swinging jets can give EVPA rotations in opposite directions within the same source (Fig. 2, change in oscillating angle from $\pi/2$ back to $-\pi/2$).
- Circularly moving and swinging jets can produce EVPA rotations with amplitude $\leq \pi/2$, including complex changes if a jet experiences only slight changes in its direction.

We stress that these very complicated, apparently random, and yet correlated variations of intensity, polarization fraction and EVPA swings come from the assumed highly regular jet motion and very regular jet structure. Most importantly, we assumed *constant* jet emissivity. We expect that variations in the acceleration/emissivity properties of the jets will further complicate the observed properties. As well as more complicated trajectories of a beam can give more complicated profiles.

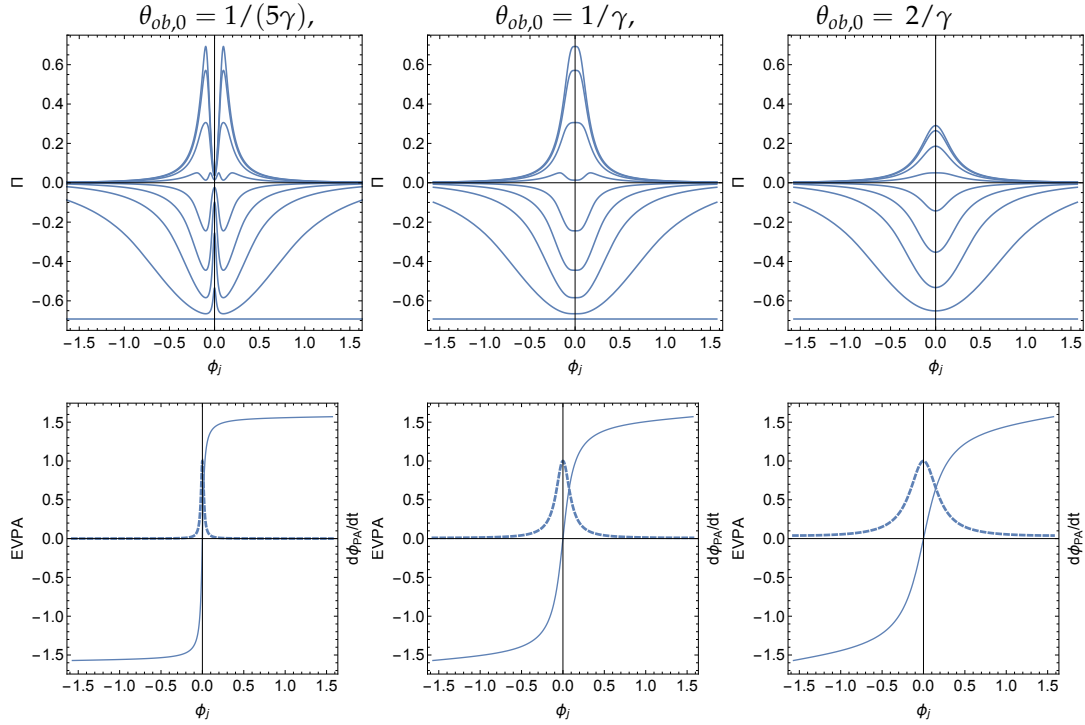


Figure 2. Polarization Π and EVPA for a jet executing planar motion. The jet is moving with bulk Lorentz factor $\gamma = 10$ and is viewed at the minimal viewing angles of $\theta_{ob,0} = 1/(5\gamma)$, $1/\gamma$, $2/\gamma$ (left to right columns). *Top Row:* Π as function of the oscillation angle for different intrinsic pitch angles (pitch angles are $0, \pi/16/\pi/8 \dots \pi/2$). *Bottom Row:* EVPA as function of the oscillation angle (solid line). Here a larger range of angles ϕ_j is plotted to show the full periodic behavior of EVPA. Dashed line: the rate of change of EVPA, $\dot{\phi}_{PA}$ (defined here as the projection of the jet on the plane of the sky - EVPA may differ by 90°), normalized to the maximal value.

3. Knots as emission patterns in swinging AGN jets

Blazar jet often show emission features that are moving along non-ballistic trajectories [12]. Lyutikov & Kravchenko (in preparation) discuss a kinematic model of the emission features as disturbances propagating along a ballistically moving jet.

Let a jet moving ballistically with velocity β_j oscillate in the $x - z$ plane. In addition, let an emitting element propagate along the jet with velocity β'_{em} with respect to the jet. In the observer frame the velocity of the element is given by relativistic addition of the radial fluid outflow and velocity along the jet, Fig. 1.

We assume that the intrinsic knot emission is constant, so that the observed flux is determined exclusively by the effects of relativistic Doppler boosting; which we assume $\propto \delta^4$, where

$$\delta = \frac{1}{\gamma(1 - \beta \cos \theta)}, \quad (1)$$

θ is the angle between the knot velocity and the line of sight, and γ is the Lorentz factor of the knot. Selected knot trajectories are pictured in Fig. 4.

3.1. Properties of emission patterns

Motion of the emission feature is the combination of advection with the ballistic jet motion and propagation along the jet. There are two qualitatively different trajectories: advection-dominated and pattern-propagation-modified regimes. In the advection-dominated regime a given feature is mostly advected with flow, moving along a nearly ballistic trajectory. In the pattern-propagation-modified

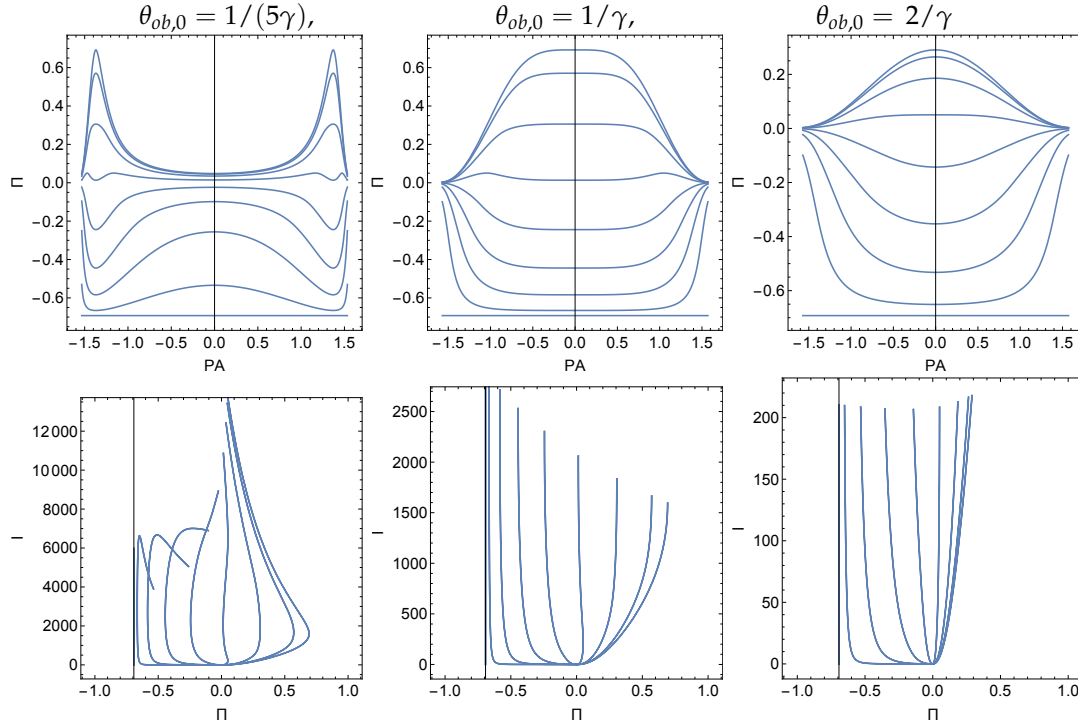


Figure 3. Same set-up as Fig. 2. *Top Row:* polarization Π as function of position angle. *Bottom Row:* Intensity as function of polarization degree Π .

regime a feature mostly follows a curved structure of the jet. Fig. 1 demonstrates that as the jet propagates further away from the launching site the direction of the jet becomes more and more perpendicular to the jet motion. Thus, qualitatively, for the pattern speed with respect to the jet of the order of the speed of light, for $\theta_{\max}\gamma_j \geq 1$ a pattern is mostly advected with the flow. On the other hand for $\theta_{\max}\gamma_j \leq 1$ a pattern can propagate through a number of different wiggles.

Analyzing the figures 4 we come to the following conclusion:

- motion of emission knots is non-ballistic;
- motion of emission knots is confined within a fixed cone; the opening angle of the cone θ_{open} is determined by the amplitude of oscillations and the viewing angle (due to small viewing angle the opening angle of knots' motion is generally much larger than the oscillations angle, $\theta_{\text{open}} \sim \theta_{\max} / \sin \theta_{\text{ob}}$);
- knots may experience seemingly sudden changes of direction (top right panel); such sudden changes are usually accompanied by brightness changes
- depending on the parameter $\theta_{\max}\gamma_j$ knots experience smooth curved trajectories that seemingly asymptotically approach straight lines (e.g., top left panel, $\theta_{\max}\gamma_j = 1.7$) or oscillatory behavior (e.g., top right panel, $\theta_{\max}\gamma_j = 0.36$)
- for cases $\theta_{\max}\gamma_j \geq 1$ typical trajectories “bend-in” - knots are moving toward the symmetry axis (top right); for $\theta_{\max}\gamma_j \leq 1$ some trajectories “bend-out”
- for high Mach numbers symmetric case (top left panel) blobs propagating along the average jet direction are brighter
- blobs may seem to appear not at the core, with seemingly non-ballistic trajectories; knots may also seem to disappear in flux limited observations (top right and bottom left panel)
- At a given projected location identical knots may have very different brightness (points of intersection of sequences of small and large circles)
- Motion of knots can be asymmetric with respect to the projection of the average direction of motion on the sky: the brightest blobs propagate along a direction which is different from the jet axis (bottom rows).

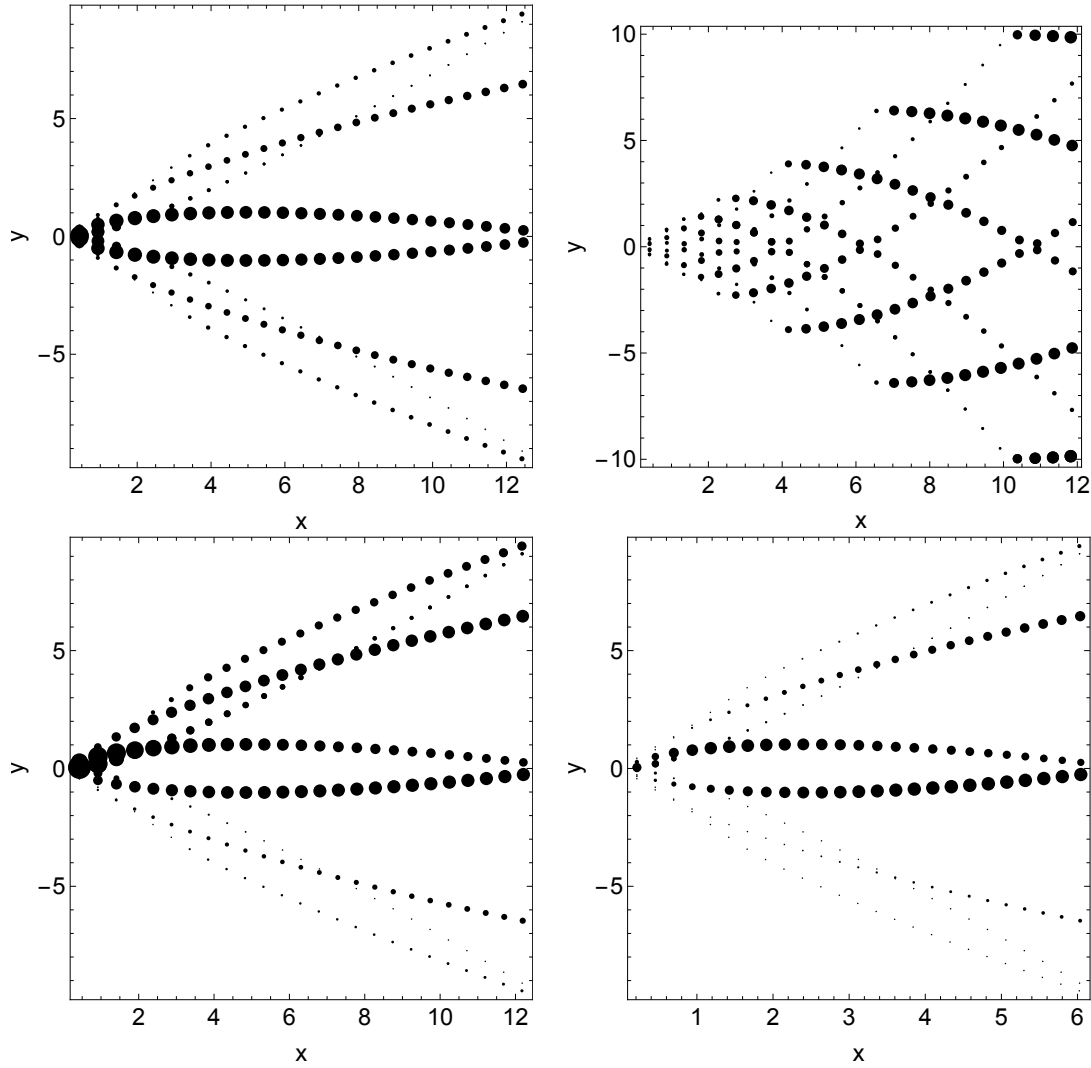


Figure 4. Examples of knot trajectories. Each panel shows 8 trajectories, corresponding to launching moments separated by an eighth of a period. The size of the circles is proportional to δ^4 (normalization is different in different panels). Projection of the central axis of the jet onto the plane of the sky is along x axis. Position of the knots are plotted for a fixed interval of the coordinate time (not observer time). Top row: $\theta_{ob} = 1/10$, $\phi_{ob} = 0$, $\mathcal{M}_j = 50$, $\gamma_j = 17$ (top left) and $\mathcal{M}_j = 10$, $\gamma_j = 3.7$ (top right). Bottom left panel: $\theta_{ob} = 1/10$, $\phi_{ob} = 1/5$, $\gamma_j = 17$, bottom right panel: $\theta_{ob} = 1/20$, $\phi_{ob} = 1/4$, $\gamma_j = 17$ (\mathcal{M}_j is the Mach number of the jet in terms of the pattern velocity).

We stress that these highly variable features come from *constant intrinsic knot emissivity*.

4. Discussion

We have outlined a model of blazar activity - a jet carrying helical magnetic field with a regularly changing direction. We demonstrate that this highly deterministic model can produce highly variable polarization, EVPAs, and intensity profiles. At the same time the model reproduces smoothly varying EVPA changes. Thus, though for any given configuration the intensity, polarization and the EVPA are deterministic and thus their behavior is highly correlated, the non-monotonic variations of these values as functions of the jet direction and Lorentz factor produce highly variable overall behavior. We find that for smooth variation of EVPA (i) Π can be highly variable; (ii) $\Pi \sim 0$ at the moment of fastest EVPA swing; (iii) the intensity is usually maximal at points of fastest EVPA swing, but can

have a minimum; (iv) for some special pitch angles there are large fluctuations of EVPA, but this always occurs at small Π .

Importantly, these features are obtained for the assumed *constant* intrinsic jet emissivity. Variations in the acceleration/emissivity properties of the jets, more complicated or irregular beam trajectories, as well as existence of multiple emission components within one beam will complicate observed profiles. In addition to the possible presence of a turbulent magnetic fields, these features may produce small ($<90^\circ$), seemingly random EVPA variations [e.g., 7]. Such variations are often observed during the quiescent state of the source and are not considered in this paper.

Bibliography

1. Lister, M.L.; Homan, D.C. MOJAVE: Monitoring of Jets in Active Galactic Nuclei with VLBA Experiments. I. First-EPOCH 15 GHz Linear Polarization Images. *AJ* **2005**, *130*, 1389–1417, [[arXiv:astro-ph/0503152](#)].
2. Lyutikov, M.; Pariev, V.I.; Gabuzda, D.C. Polarization and structure of relativistic parsec-scale AGN jets. *MNRAS* **2005**, *360*, 869–891.
3. Gabuzda, D.C. VSOP observations of the compact BL Lacertae object 1803+784. *NAR* **1999**, *43*, 691–694.
4. Pushkarev, A.B.; Gabuzda, D.C.; Vetukhnovskaya, Y.N.; Yakimov, V.E. Spine-sheath polarization structures in four active galactic nuclei jets. *MNRAS* **2005**, *356*, 859–871.
5. Quirrenbach, A.; Witzel, A.; Krichbaum, T.; Hummel, C.A.; Alberdi, A. Rapid variability of extragalactic radio sources. *Nature* **1989**, *337*, 442–444.
6. Ulrich, M.H.; Maraschi, L.; Urry, C.M. Variability of Active Galactic Nuclei. *ARA&A* **1997**, *35*, 445–502.
7. Larionov, V.M.; Jorstad, S.G.; Marscher, A.P.; Morozova, D.A.; Blinov, D.A.; Hagen-Thorn, V.A.; Konstantinova, T.S.; Kopatskaya, E.N.; Larionova, L.V.; Larionova, E.G.; Troitsky, I.S. The Outburst of the Blazar S5 0716+71 in 2011 October: Shock in a Helical Jet. *ApJ* **2013**, *768*, 40, [[arXiv:astro-ph.HE/1303.2218](#)].
8. Marscher, A.P.; Jorstad, S.G.; D’Arcangelo, F.D.; Smith, P.S.; Williams, G.G.; Larionov, V.M.; Oh, H.; Olmstead, A.R.; Aller, M.F.; Aller, H.D.; McHardy, I.M.; Lähtenmäki, A.; Tornikoski, M.; Valtaoja, E.; Hagen-Thorn, V.A.; Kopatskaya, E.N.; Gear, W.K.; Tosti, G.; Kurtanidze, O.; Nikolashvili, M.; Sigua, L.; Miller, H.R.; Ryle, W.T. The inner jet of an active galactic nucleus as revealed by a radio-to- γ -ray outburst. *Nature* **2008**, *452*, 966–969.
9. Kiehlmann, S.; Savolainen, T.; Jorstad, S.G.; Sokolovsky, K.V.; Schinzel, F.K.; Marscher, A.P.; Larionov, V.M.; Agudo, I.; Akitaya, H.; Benítez, E.; Berdyugin, A.; Blinov, D.A.; Bochkarev, N.G.; Borman, G.A.; Burenkov, A.N.; Casadio, C.; Doroshenko, V.T.; Efimova, N.V.; Fukazawa, Y.; Gómez, J.L.; Grishina, T.S.; Hagen-Thorn, V.A.; Heidt, J.; Hiriart, D.; Itoh, R.; Joshi, M.; Kawabata, K.S.; Kimeridze, G.N.; Kopatskaya, E.N.; Korobtsev, I.V.; Krajci, T.; Kurtanidze, O.M.; Kurtanidze, S.O.; Larionova, E.G.; Larionova, L.V.; Lindfors, E.; López, J.M.; McHardy, I.M.; Molina, S.N.; Moritani, Y.; Morozova, D.A.; Nazarov, S.V.; Nikolashvili, M.G.; Nilsson, K.; Pulatova, N.G.; Reinthal, R.; Sadun, A.; Sasada, M.; Savchenko, S.S.; Sergeev, S.G.; Sigua, L.A.; Smith, P.S.; Sorcia, M.; Spiridonova, O.I.; Takaki, K.; Takalo, L.O.; Taylor, B.; Troitsky, I.S.; Uemura, M.; Ugolkova, L.S.; Ui, T.; Yoshida, M.; Zensus, J.A.; Zhdanova, V.E. Polarization angle swings in blazars: The case of <ASTROBJ>3C 279</ASTROBJ>. *A&A* **2016**, *590*, A10, [[arXiv:astro-ph.HE/1603.00249](#)].
10. Blandford, R.D.; Königl, A. Relativistic jets as compact radio sources. *ApJ* **1979**, *232*, 34–48.
11. Lyutikov, M.; Pariev, V.I.; Blandford, R.D. Polarization of Prompt Gamma-Ray Burst Emission: Evidence for Electromagnetically Dominated Outflow. *ApJ* **2003**, *597*, 998–1009, [[astro-ph/0305410](#)].
12. Lister, M.L.; Aller, M.F.; Aller, H.D.; Homan, D.C.; Kellermann, K.I.; Kovalev, Y.Y.; Pushkarev, A.B.; Richards, J.L.; Ros, E.; Savolainen, T. MOJAVE: XIII. Parsec-scale AGN Jet Kinematics Analysis Based on 19 years of VLBA Observations at 15 GHz. *AJ* **2016**, *152*, 12, [[1603.03882](#)].